White Rose Research Online

eprints@whiterose.ac.uk
https://eprints.whiterose.ac.uk
Universities of Leeds, Sheffield and York

Deposited via The University of Sheffield.

White Rose Research Online URL for this paper:
https://eprints.whiterose.ac.uk/id/eprint/193745/

Version: Accepted Version

Article:
Wang, L.G., Pradhan, S.U., Wassgren, C. et al. (2020) A breakage kernel for use in population balance modelling of twin screw granulation. Powder Technology, 363. pp. 525-540. ISSN: 0032-5910

https://doi.org/10.1016/j.powtec.2020.01.024

Article available under the terms of the CC-BY-NC-ND licence (https://creativecommons.org/licenses/by-nc-nd/4.0/).

Reuse
Items deposited in White Rose Research Online are protected by copyright, with all rights reserved unless indicated otherwise. They may be downloaded and/or printed for private study, or other acts as permitted by national copyright laws. The publisher or other rights holders may allow further reproduction and re-use of the full text version. This is indicated by the licence information on the White Rose Research Online record for the item.

Takedown
If you consider content in White Rose Research Online to be in breach of UK law, please notify us by emailing eprints@whiterose.ac.uk including the URL of the record and the reason for the withdrawal request.

UNIVERSITY OF LEEDS
University of Sheffield
UNIVERSITY of York

A breakage kernel for use in population balance modelling of twin screw granulation

Li Ge Wang[a1], Shankali U. Pradhan[b1], Carl Wassgren[c], Dana Barrasso[d], David Slade[e], James D. Litster[a]*

[a]School of Chemical and Biological Engineering, University of Sheffield, UK

[b]Davidson School of Chemical Engineering, Purdue University, USA

[c]School of Mechanical Engineering, Purdue University, USA

[d]Process Systems Enterprise, New Jersey Office, USA

[e]Process Systems Enterprise, Hammersmith, London, UK

[1] Joint first authors

Email: James.Litster@sheffield.ac.uk

Abstract

This paper presents a novel breakage kernel for use in population balance modelling for twin screw granulation using a mechanistic understanding in different screw elements. Breakage-isolated experiments are conducted using conveying and distributive mixing elements for a range of model formulations of widely different yield stresses. The breakage kernel, i.e. the selection and breakage functions, are mathematically formed based on the identification of the dominant breakage mechanisms of chipping and fragmentation in the conveying and distributive mixing elements, respectively, and the unique geometries of the two screw elements. A parametric study for the proposed breakage kernel is performed to identify the influential parameters on the breakage kernel. This is the first breakage model specifically developed for a TSG and incorporates a mechanistic understanding of several key parameters, particularly the role of screw geometry. The breakage model is well suited to population balance modelling framework for model-driven design of twin screw granulation.

Keywords: Breakage kernel, Population balance model, Critical breakage size, Screw geometry, Twin screw granulation

1 Introduction

Wet granulation is a key component in the integration of continuous pharmaceutical manufacturing. As an emerging technology for continuous wet granulation, twin screw granulation is becoming increasingly popular due to its large material throughput, flexible screw configuration, short residence time, and small capital costs. Hence, there has been considerable interest in the study of twin screw granulation both experimentally and numerically.

A twin screw granulator consists of two intermeshed co-rotating screws encased in a barrel with powder and liquid injection ports. The positions of the powder and liquid injection ports can be adjusted easily. The screws are assembled using individual screw elements available in different screw geometries. The material is conveyed along the length of the screw and granulation occurs by mechanical mixing of the powder and the granulating liquid in the granulator.

Several mechanistic studies have been conducted in twin screw granulators to understand governing rate processes. A twin screw granulator operates in the mechanical dispersion regime, relying on mixing elements to disperse a liquid throughout the powder mass [1,2]. Thus, granule breakage has been shown to be a key rate process affecting granule properties since breakage is necessary for good liquid distribution [3].

Granule breakage varies considerably with different screw geometries, resulting in a variety of granule properties. It has been shown that conveying elements primarily transport material and cause minor attrition of granules. Conveying elements do not cause intense mixing of the powder and the binder [1,4–6], resulting in a bimodal distribution of granules marked by a fines mode in the granule size distribution corresponding to ungranulated material [4,7,8]. Kneading elements cause intense mixing of material by shearing and extruding the wet mass, resulting in dense granules with flat, elongated shapes [9–12]. Distributive mixing elements also cause intense mixing of the wet mass via a chopping and fragmentation breakage mechanism [3-6, 13, 14]. As a result, the granules from distributive mixing elements are more porous compared to kneading elements and rounder in shape. Since twin screw granulators have a small free volume compared to high shear or fluidized bed granulators, screw geometry plays an important role in controlling the maximum

granule size that can be produced. The maximum granule size can be obtained by estimating the largest sphere that can fit in the free volume of a given screw geometry [4, 5, 15]. The maximum granule size in a conveying element is set by the space available between the two flights of the conveying element and barrel whilst the maximum granule size in a distributive mixing element is the space between the teeth of the elements and the barrel [5].

Granule size, shape, and porosity are sensitive to formulation properties (such as API and excipient type, blend particle size distribution, binder viscosity, etc.), process parameters (such as material feed rate, liquid to solid ratio, and screw speed), and screw element geometry [1, 2, 4, 5, 11, 13, 16, 34]. Hence, it is important to understand the effect of formulation properties and process parameters on granule breakage with different screw geometries. The breakage of a wet granule depends on its dynamic yield strength (DYS), which describes the mechanical behaviour of the wet mass. The DYS is dependent on the primary powder particle size, binder viscosity and surface tension, powder binder contact angle, granule porosity and saturation, and strain rate of deformation [35-37]. The material feed rate and screw speed are the key process parameters affecting the granule properties in a twin screw granulator. The interlinked effects of material feed rate and screw speed are captured by the dimensionless Powder Feed Number (PFN) given by [23]:

$$PFN = \frac{\dot{m}_{powder}}{\rho_{bulk}\omega D^3} \quad (1)$$

where $\dot{m}_{powder}$ is the powder feed rate in the granulator, ρ_{bulk} is the powder poured bulk density, ω is the screw speed, and D is the screw diameter.

The material fill level in the granulator is directly proportional to the PFN. Some studies reported in the literature show that the PFN does not have a statistically significant effect on granule properties [23]. However, some reports have suggested that increasing the material fill level in the granulator increases the mean granule size [8, 14, 31]. As a result, the precise effect that the PFN has on granule breakage remains uncertain.

Population balance modelling is recognized to be a powerful model-based design tool for understanding the prediction and optimization of continuous twin screw granulation processes. For example, Paavola et al. [38] defined two rate process kernels, i.e., consolidation and aggregation, to study the size, porosity, and saturation distributions of

granules. However, growth behaviour by layering and breakage is omitted in their study. Barrasso et al. [39] used a multi-dimensional population balance model for continuous twin screw granulation where the rate processes of aggregation, breakage, liquid addition, and consolidation were taken into account. The influence of liquid-to-solid ratio was studied and larger liquid addition rates resulted in higher frequencies of larger particles as well as a reduction in primary particles. Likewise, a population balance model-based analysis of twin screw granulation was carried out for continuous solid dosage manufacturing by Kumar et al. [40]. A 1D population balance model was adopted with aggregation and breakage in the kneading elements. Unknown input parameters were estimated using the experimentally-measured particle size distribution. Recently, the spatial heterogeneity in twin screw granulation was evaluated with a three-compartment population balance model by Liu et al. [41]. The three compartments were composed of wetting (conveying), mixing (kneading), and steady growth (conveying) sections. Within these compartments it was assumed that aggregation occurred in the wetting compartment and breakage occurred in the mixing elements. Aggregation and breakage took place in the steady growth compartment.

As inferred from the preceding discussion, one of the main challenges of population balance modelling is development of a reasonable model where the rate process kernels are defined based on the screw configuration. Although several breakage kernels have been used in population balance models [39, 48], there have been two main deficiencies in their formulation. First, the breakage mechanisms are not properly characterised in different screw elements and the majority of existing breakage kernels use the same function regardless of the screw type. Second, a mechanistic-based breakage kernel is yet to be established for twin screw granulation where the process parameters and mechanical properties of the particles are incorporated into the breakage probability function.

This paper develops new breakage kernels for use in population balance modelling of twin screw granulation. To characterise the breakage mechanism within the twin screw granulator, breakage-isolated experiments are performed using conveying and distributive mixing element configurations. Breakage experiments for kneading elements are out of the scope of this paper. We recommend similar studies on different configurations of kneading elements (e.g., 30^{o} forward, 30^{o} reverse, 60^{o} forward, 60^{o} reverse, and 90^{o}) to gain insight into the shearing mechanisms associated with kneading elements. From the experimental

observations, the dominant breakage mechanisms are identified as chipping and a combination of chipping and crushing for the conveying and distributive mixing elements, respectively. The selection and breakage functions are mathematically formed as functions of the powder feed number (PFN), dynamic yield strength (DYS), and screw element geometry. These new breakage kernels improve the population balance modelling of twin screw granulation by providing mechanistic-based breakage kernels that are screw configuration dependent.

2 Population balance model for twin screw granulation

Population balance modelling has been widely used to track granule attribute evolution in twin screw granulation. The dimension of the population balance model is dependent on the number of phases (solid, liquid, and gas) to be considered. Most population balance models in the literature are one-dimensional, usually considering only the variation of particle size or volume. One-dimensional population balance models fall short of predicting all granule properties of interest due to their inability to track granule-to-granule variation in liquid content and granule porosity. Therefore, 3D population balance models have been developed to account for the variations in solid, liquid, and gas composition. Most granulation population balance models include rate process kernels for consolidation, aggregation, and breakage. The development of breakage kernels is the focus of this paper.

2.1 Governing equations of population balance model

Multi-dimensional population balance models (PBMs) have been developed to track granule solid, liquid, and gas volumes. A typical 3D population balance model may be written as [42]:

$$\frac{\partial}{\partial t}n(s,l,g,t)+\frac{\partial}{\partial s}\left[n(s,l,g,t)\frac{ds}{dt}\right]+\frac{\partial}{\partial l}\left[n(s,l,g,t)\frac{dl}{dt}\right]+\frac{\partial}{\partial g}\left[n(s,l,g,t)\frac{dg}{dt}\right] = B_{nuc}(s,l,g,t)+B_{break}(s,l,g,t)-D_{break}(s,l,g,t)+B_{lay}(s,l,g,t) \quad (2)$$

where (s,l,g) is the vector representing the solid, liquid, and gas volumes of a granule and $n(s,l,g,t)$ is the population density of a granule with these three components over time. The three non-temporal partial differential terms refer to the state change due to solid layering, liquid addition, and gas consolidation, respectively. The quantities $B_{nuc}(s,l,g,t)$

and $B_{lay}(s,l,g,t)$ denote the net rates of nucleation and layering, respectively. The terms $B_{break}(s,l,g,t)$ and $D_{break}(s,l,g,t)$ denote the birth and death rates due to breakage.

2.2 Rate expression for breakage

The population balance model shown in Eq. (2) is a framework to track the granule volume development considering three phases, i.e., solid, liquid, and gas. Breakage events are a function of factors such as the granule properties (size, shape, porosity, mechanical properties, etc.) and the operational variables. It is assumed that broken granules will have the same composition as the original granule. Therefore, we can write the breakage equations in one internal dimension, with the granule size evolution as a function of the aforementioned factors,

$$D_{break}(v) = S(v)n(v,t) \tag{3}$$

where $S(v)$ is the specific breakage rate of granules of volume v and $v = s + l + g$.

A granule of volume v can be created from the breakage of a larger-sized granule of volume w. Hence, the birth term of a granule is,

$$B_{break}(v) = \int_v^\infty S(w)b_M(v,w)M(v,t)dw \tag{4}$$

where $S(w)$ is the specific breakage rate of the mass fraction of granules of volume w.

When breakage is the only rate process, the population balance model for the mass-based breakage equation can be derived by combining Eqs. (2), (3), and (4) [43],

$$\frac{dM(v,t)}{dt} = \int_v^\infty S(w)b_M(v,w)M(v,t)dw - S(v)M(v,t) \tag{5}$$

where $M(v,t)$ is the mass of granules with volume v at time t. The breakage function $b_M(v,w)$ denotes the breakage size distribution probability between the volume range v and w, with $b_M(v,w) = B_{w,v} - B_{w-1,v}$ where B is the cumulative distribution of particle in different size fractions.

The breakage kernel is composed of two important functions: the selection function (S) and breakage function (B_m). The selection function represents the breakage rate of granules

whilst the breakage function represents the size distribution after breakage. The development of the selection and breakage functions for conveying and distributive mixing elements are described in the following sections.

3 Experimental protocol

Prior studies on twin screw granulation (TSG) focus on understanding the effects of screw configuration, formulation properties, and process properties on granule attributes [2]. However, granule properties are controlled by several rate processes. In order to understand the governing factors for granule breakage in a TSG, novel experiments that isolate breakage from other granulation rate processes were carried out using conveying (CE) and distributive mixing element (DME) configurations [44]. The experimental protocol and granule breakage probability and daughter size distribution measurements have been previously reported [5]; however, the setup of the breakage-isolating experiments is briefly described here for the reader's convenience.

3.1 Materials

To understand the influence of screw element geometry on breakage probability for different granule sizes, breakage experiments were first conducted using Play Doh (Hasbro Inc., USA) spheres of different diameters. For the CEs, Play Doh spheres with diameters of 1.0 ± 0.1 mm, 2.0 ± 0.1 mm, 3.0 ± 0.1 mm, and 4.0 ± 0.1 mm were prepared. For the DMEs, spheres of diameter 1.0 ± 0.1 mm, 2.0 ± 0.1 mm, and 3.0 ± 0.1 mm were prepared. Twenty Play Doh spheres were prepared for each diameter.

The effects of material properties and process parameters on granule breakage characteristics were studied using pellets prepared from model powders and liquid binders. Glass ballotini (Potters Industries LLC, OH, USA) with five size ranges, i.e., 0-10 µm, 63-90 µm, 125-128 µm, 180-250 µm, and 355-500 µm, were selected as the model powder material due to its well-controlled properties. A Malvern Mastersizer 2000 (Malvern, UK) was used to measure the size distribution of the glass ballotini using water as the wet dispersing medium. The particle size distribution of the glass ballotini with the aforementioned five size ranges can be found elsewhere [44]. Two model binders of different viscosities were used, namely, silicone oil (Sigma-Aldrich Corp, MO, USA) and a glycerol solution (Sigma-Aldrich Corp., MO, USA), the viscosities of which were 64 Pa.s and 0.7 Pa.s, respectively. Twenty cylindrical

pellets (diameter = height) were prepared for each model material system, having diameters of 2 mm and 3 mm, using a Natoli punch and die set and an Instron ElectroPlus E1000 to punch the pellets. Two replicate breakage experiments were performed for the 3 mm pellets in conveying and distributive mixing elements, and 2 mm pellets in distributive mixing elements as summarized in Table 1. The details of the pellet preparation method are described in previously published work [5]. It is important to note that breakage is a probabilistic process and a statistically significant number of pellets should be used to account for the randomness in the breakage of the pellets. In this work, we have not explored the effect of sample size of feed pellets on the scatter in the data. A sample size of twenty feed pellets was used. It is worth noting that previously published breakage-only experiments in high shear granulation literature have also used twenty feed pellets for each experiment [50, 51]. For future studies, we recommend performing studies with a larger sample size to refine the data.

The dynamic yield strength (DYS) of Play Doh and the model materials was measured using an Instron ElectroPlus E1000. As discussed in Section 1, the mechanical behaviour of wet granules resembles an elasto-plastic material. The material undergoes elastic deformation until the stress reaches the dynamic yield strength value, following which, the material plastically deforms and the granule is considered broken [45]. The details and results of the dynamic yield strength measurement are given in a previous publication [5].

3.2 Breakage-isolating experiments

The breakage-isolating experiments [5] were carried out in a Thermo Fisher Scientific EuroLab 16 mm Twin Screw Granulator with 25:1 length-to-diameter. The TSG barrel length is 380 mm and is composed of six 60 mm zones and one 20 mm zone at the end. A combination of conveying and distributive mixing elements are used in the experiments. The experimental set up is shown in Figure 1. For the CE breakage experiments, all six 60 mm zones and the 20 mm zone are comprised of conveying elements. Both the powder and the pellet are fed from zone 4 for the CE breakage specific experiments. For the DME breakage experiments, the six 60 mm zones are comprised of conveying elements and the 20 mm zone consists of the three DME pairs and a part of the adjacent conveying element. For the DME experiments, the powder is fed from zone 4 whilst the pellet is fed from an aperture in the middle of the 20 mm section in front of zone 1 to ensure that the pellets only

Deleted:

experience the DME zone. In all of these experiments microcrystalline cellulose (MCC) was used as the surrounding free flowing carrier powder medium to simulate the powder fill in the twin screw granulator. The powder feed number (given in equation 1) incorporates the feed rate of MCC in the granulator and the screw speed to evaluate the effects of process parameters on the breakage behaviour in conveying and distributive mixing elements.

Figure 1. Schematic of the experimental setup using conveying and distributive mixing elements (reproduced from Pradhan et al. [5])

The experiments were performed at three screw speeds (200 RPM, 400 RPM, and 800 RPM) and two MCC feed rates (2 kg/h and 4 kg/h), which results in three different powder feed numbers (PFN = 0.011, 0.022, and 0.045) [23].

For 3 mm pellets in conveying elements, previously performed work [5] showed that the breakage probability at a PFN of 0.022 (resulting from a screw speed of 400 RPM and powder feed rate of 4 kg/h, as given by equation 1) was a function of the material DYS. Hence, breakage experiments at low and high PFN were performed to understand the effects of process parameters on the breakage probability. Furthermore, an additional breakage experiment was performed at the center point PFN of 0.022, albeit using different individual values of the screw speed and powder feed rate to investigate if the results depend on individual values of the process parameters.

We have previously shown that 2 mm pellets in conveying elements did not show breakage at a PFN of 0.022 [5]. Hence, the breakage experiment was performed at a larger value of PFN (and, thus, a larger fill level in the granulator) to understand if doubling the fill enhances breakage.

Likewise, breakage experiments for 2 mm pellets in distributive mixing elements were performed at low, center point, and high PFNs, and an additional experiment was performed at a PFN of 0.011 but with different values of the individual screw speed and powder feed rate. For 3 mm pellets in distributive mixing elements, previously performed breakage experiments at the center point PFN showed complete breakage of the pellets regardless of material strength [5]. Hence, an additional breakage experiment was

performed at a low PFN to observe if lowering the PFN results in a reduction of breakage for the 3 mm pellets.

The experimental design of the breakage experiments using model granular materials is summarized in Table 1.

The pellet remnants and the MCC powder were collected at the outlet of the granulator for breakage probability and breakage fragment distribution analysis. The breakage probability was measured by counting the number of survivor pellets out of the twenty feed pellets. Each broken pellet constitutes a 5% breakage probability. The breakage size distribution was measured using a $\sqrt{2}$ series of sieves from 0.5 mm to 2.8 mm.

Table 1. Experimental design of the breakage specific experiments in CEs and DMEs

3.3 Results

In this section, the results from the breakage-isolating experiments that are used to develop the breakage kernels are described. The experiments focused on the influence of material properties and screw element geometry on the breakage probability and daughter size distribution have been previously published [5]. The following section describes the development of a breakage kernel using this previously published data [5] and additional experimental data.

3.3.1 Breakage probability in conveying elements

The effect of granule size on breakage probability was first investigated in CEs with a PFN equal to 0.022 using Play Doh spheres. The breakage probability results for the Play Doh spheres from three replicates are shown in Figure 2.

Figure 2. Breakage probability of a Play Doh sphere as a function of size in CEs (reproduced from Pradhan et al. [5])

There is no breakage for a sphere smaller than 3 mm while a 4 mm sphere has a 100% breakage probability. For the elements used in the experiments described in this paper, the maximum granule size in the CEs was 3.49 mm as measured using CAD analysis [5].

Deleted:

Deleted:

Considering the calculated maximum sphere size is 3.49 mm in CEs, it is expected that the breakage probability would be 100% above this critical value.

The effect of material properties and process parameters on granule breakage was measured using model material pellets of different DYS values, of size 2 mm and 3 mm, as per the experimental design in Table 1. The breakage probabilities of 3 mm and 2 mm pellets are plotted as a function of DYS for varying PFN for CEs in Figure 3 and Figure 4. In Figure 3, the breakage probability of a 3 mm pellet decreases when the DYS is increased until 9 kPa. The breakage probability drops to almost zero when the pellets are stronger than 9 kPa irrespective of the operating conditions. The breakage probability increases with increasing PFN, particularly for weaker materials, i.e., smaller DYS values. It is worth noting that the breakage probability is similar for the same PFN, even though the screw RPM and mass flow rate are different. It is important to note that one broken pellet accounts for 5% breakage probability and, considering the probabilistic nature of granule breakage, small differences observed in the data for the same PFN can arise from the randomness of the breakage itself. There is no breakage of 2 mm granules regardless of the DYS and PFN (Figure 4). The weakest material shows a 5% breakage probability for a PFN of 0.022. However, we consider this point as an outlier because the same material showed zero breakage for a larger PFN and, thus, a larger fill level. The weakest material is subject to the largest scatter in the data because the material strength is low.

The most important parameter in determining granule breakage is the size of the granule. All granules greater than the geometrically determined maximum size (3.49 mm) break. Just below the critical size (3 mm), granule breakage is a function of granule strength (DYS) and powder flow number (PFN). Well below the critical size (2 mm), no breakage occurs regardless of material properties and process parameters.

Figure 3. Breakage probability of 3 mm pellets as a function of DYS for varying PFN using CEs

Figure 4. Breakage probability of 2 mm pellets as a function of DYS for varying PFN using CEs

Deleted:

Deleted:

Deleted:

Deleted:

3.3.2 Breakage probability in distributive mixing elements

Figure 5 shows the breakage probability of the Play Doh spheres as a function of size at a screw speed 400 RPM and powder feed rate of 4 kg/h (PFN=0.022) [5]. The breakage probability in DMEs increases gradually from 0 to 100% breakage as size increases from 1 mm to 3 mm. In contrast, the breakage probability in CEs over the size range from 1 mm to 3 mm is observed to be nearly zero. The maximum granule size in the DMEs is 3.19 mm using a CAD model analysis [5]. The DME breakage probability is 100% at 3 mm, which is close to the predicted critical size, confirming that the breakage pattern is strongly screw geometry dependent.

Figure 5. Breakage probability of Play Doh spheres as a function of particle size in DME (reproduced from Pradhan et al. [5])

The model material breakage specific experiments in DMEs were carried out using 2 mm and 3 mm pellets. The breakage probability of the 2 mm model materials as a function of DYS is given in Figure 6 for three PFNs (as described in Table 1). Similar to the CEs, the breakage probability increases with decreasing DYS and increasing PFN. The influence of PFN is more pronounced for weaker materials.

Figure 6. Breakage probability of 2 mm pellets as a function of DYS for varying PFN using DMEs

Figure 7 displays the breakage probability of 3 mm pellets as a function of DYS and PFN. The breakage probability is 100% irrespective of the DYS and PFN. This result is due to the 3 mm pellets being at approximately the DME geometric limit and, thus, are subject to fragmentation.

Figure 7. Breakage probability of 3 mm pellets as a function of DYS for varying PFN using DMEs

For both CEs and DMEs, the breakage probability is a function of PFN, DYS, and granule size. Granules at or above the maximum critical size will break. For granules slightly smaller than

the maximum critical size, the breakage probability increases with decreasing DYS and increasing PFN. In particular, the effect of PFN is more pronounced for the weaker materials. Small granules do not break, independent of material properties and process conditions. The breakage pattern is observed to be strongly screw geometry dependent. Any mechanistic TSG breakage kernel should be consistent with these findings. In particular, we expect the breakage kernel must be screw element specific.

3.3.3 Breakage fragment size distribution

The breakage fragment size distributions of pellets broken in CE and DME elements have been reported in a previous study [5]. It was concluded from those breakage fragment distributions that chipping and fragmentation were the dominant breakage mechanisms in the conveying elements and distributive mixing elements, respectively. Here, the daughter size distribution in each screw element is presented and will be used to model the breakage function. The data points shown are the average of two replicate measurements with the scatter bars showing the range. For each replicate, the pellets with five ranges of DYS are sampled and collected for breakage fragment size measurement. There are 10 datasets for CEs and 16 datasets for DMEs in two replicates. The data for the individual replicates is provided in the supplementary information. The large scatter bars are due to the randomness of granule breakage and the small masses in each sieve cut. The breakage size distributions of 3 mm pellets in CEs and DMEs are shown in Figure 8 and Figure 9, respectively. The PFN for the CE data is 0.045 at a feed rate of 4 kg/h and screw speed of 200 RPM while the PFN for the DME data is 0.022 at a feed rate of 4 kg/h and screw speed 400 RPM.

Figure 8. Breakage fragment distribution from 3 mm pellets in CEs (PFN = 0.045) (a) Mass-based particle size distribution (b) Mass-based cumulative size distribution (Data from [44])

Figure 9. Breakage size distribution of breakage particle in DMEs (PFN = 0.022) (a) Mass-based particle size distribution (b) Mass-based cumulative size distribution (data from [44])

Due to the chipping mechanism in CEs, the fragment frequency distribution in Figure 8a is bi-modal with one peak at 0.605 mm and the other peak at 2.4 mm in the size fraction immediately smaller than the parent pellet. On the other hand, Figure 9a shows the mono-

Deleted:
Deleted:
Deleted:
Deleted:

modal fragment frequency distribution for DMEs with a mode at 1.7 mm. The DMEs produce extensive granule breakage as the granule breaks into small fragments. In comparison, the CEs cause granule chipping, as indicated by the bimodal distribution. A good breakage model must capture these differences in fragment size distribution.

4 Breakage kernel development

Compared to other rate processing kernels, the published TSG breakage kernels for PBM are mainly borrowed from milling or high shear granulation, which results in a discrepancy in the type of stressing events in a TSG and, thus, inaccuracies in the prediction of granule size distributions. The findings from the breakage specific tests using the CEs and DMEs indicate that breakage probability is a function of the geometry of the screw element, PFN, and material DYS. There are currently no existing breakage kernels in TSG that capture these parameters in the selection and breakage functions. Hence, the development of TSG breakage kernels incorporating these parameters is needed in order to improve the predictive capacity of TSG PBMs. This section presents the development of selection and breakage functions based on the findings from the breakage specific experiments for the two screw elements.

4.1 Selection function (SF) development

4.1.1 Breakage pattern in TSG

Pradhan et al. [5] proposed breakage mechanisms in the TSG, i.e., chipping in CEs and fragmentation in DMEs. Chipping is subsurface material removal from the particle due to local damage, such as edge or corner detachment. Fragmentation denotes the splitting of the original particle into several pieces. Based on the results in Section 3, we propose two different functions for breakage probability as a function of size for the different element types and breakage mechanisms, shown schematically in Figure 10,

Deleted:

Figure 10. Schematic outline of two breakage patterns. (a) chipping in CEs and (b) fragmentation in DMEs

In Figure 10(a) (CE, chipping), the breakage probability increases with increasing granule size between the minimum and maximum breakage sizes. The breakage probability

Deleted:

corresponding to chipping is reported to follow a power law in the literature [46] before a sudden jump to 100% breakage due to the geometric constraints in the screw element. In Figure 10(b) (DME, fragmentation), the breakage probability increases smoothly for sizes greater than the minimum breakage size until reaching 100% at the maximum breakage size. The model is described using a Weibull law expression, which is often used for fragmentation probability distributions [46]. For both CEs and DMEs, there exist two critical sizes: the minimum breakage size x_{lc} and the maximum breakage size x_{uc}. The minimum breakage size x_{lc} is a material dependent parameter, above which particle breakage takes place. The maximum breakage x_{uc} is a screw-dependent parameter, which is defined as the largest available gap size allowing particles to pass through and remain unbroken. It should also be noted that the breakage size region (x_{lc}, x_{uc}) in DMEs is usually broader than that in CEs due to more intensive stressing events in DMEs leading to a smaller x_{lc}.

Deleted:

4.1.2 SF in conveying elements

The breakage rate S is found by multiplying the number of breakage events per unit time and the breakage probability:

$$S = N * P_x \tag{6}$$

where N is the number of breakage events per unit time (proportional to the screw speed) and P_x is the breakage probability relevant to the process parameters and particle properties [47].

The breakage probability P_x was found to increase with an increase in PFN and granule size and a decrease in DYS. Taking these parameters into account along with the upper and lower granule size limits for breakage, an empirically-derived selection function for conveying elements may be written as:

$$P_x = \begin{cases} 1 & x \geq x_{uc} \\ a * exp(-\frac{DYS}{b} * \frac{1}{PFN}) * (x/x_{uc})^c & x_{lc} < x < x_{uc} \\ 0 & x \leq x_{lc} \end{cases} \tag{7}$$

where the parameters a, b, and c are fitting constants.

The fitting results of Eq. (7) against the breakage data for 3 mm pellets of nine different model materials in the TSG with only CEs subject to two feed rates and three screw speeds are shown in Figure 11.

Deleted:

Figure 11. Predictive breakage probability vs. breakage dataset for 3 mm pellets in CEs

Relatively good agreement is observed between the predictions and data for the sets of conditions. The parameters a, b, and c for each set of data were estimated using a nonlinear least squares method in MATLAB based on a global fitting of the four data sets. Global fitting herein means the estimation of parameters a, b, and c based on the four datasets of breakage probability subject to varying rotary speed and feed rate (varying PFN as a result). This method is different from that of parameter estimation using an individual dataset, resulting in four sets of different values of a, b, and c. The decision to use global fitting is made based on the model universality to show its predictive powder applied to all of the operational conditions.

Note that the parameters a and c are combined as $\hat{a} = a * (x/x_{uc})^c$ for fitting since the pellet size is constant at 3 mm. The fitting parameters of $\hat{a}$ and b are tabulated in Table 2. The minimum breakage size for the model material x_{lc} is taken as 2 mm and the maximum breakage size x_{uc} is 3.49 mm. The confidence interval of the fitting parameters is 95% by default unless stated elsewhere.

Deleted:

Table 2. The fitting parameters of $\hat{a}$ and c in CEs

The predicted and measured breakage probabilities in Figure 11 are plotted again in Figure 12, with the measured breakage probabilities on the horizontal axis and predicted values on the vertical axis. It is observed that the majority of the data follows the 45 degree line, indicating that the proposed fit is a good one.

Deleted:

Figure 12. Fitted vs. measured breakage probability for 3 mm pellets in CEs

4.1.3 SF in distributive mixing elements

The breakage probability in DMEs is found to be a strong function of the screw geometry, DYS, and the powder feed number (PFN). We propose the following empirically-derived three parameter model for the breakage selection function in DMEs:

$$P_x = \begin{cases} 1 & x \geq x_{uc} \\ 1 - a * exp\left(-PFN * \frac{b}{DYS} * \left(\frac{x}{x_{uc}}\right)^c\right) & x_{lc} < x < x_{uc} \\ 0 & x \leq x_{lc} \end{cases} \quad (8)$$

As with Eq. (7), the parameters a, b, and c are fitting parameters.

The fitting results of Eq. (8) against the measured DME breakage data for two feed rates and three screw speeds are shown in Figure 13. The minimum breakage size is 1.0 mm based on Figure 5 and the maximum breakage size is measured as 3.18 mm from the screw element geometry. Good agreement between the predictions and the experimental data is observed. Note that the parameters b and c are combined as $\hat{b} = b * (x/x_{uc})^c$ for the fit since the pellet size is constant at 2 mm. The parameter values for a and $\hat{b}$ are summarized in Table 3 using a global fitting method based on the four DME data sets.

Figure 13. Fitted breakage probability predictions vs. measurements for 2 mm pellets in DMEs

Table 3. The fitting parameters of a and $\hat{b}$ in DMEs

Figure 14 plots the same data in Figure 13, but as the predicted breakage probability as a function of the measured breakage probability. The data following the 45 degree line indicates that the proposed fit is a good one.

Figure 14. Fitted vs. measured breakage probability for 2 mm pellets in DMEs

Note that the developed model of breakage probability has the ability to account for the breakage of granules formed by other rate processes such as coalescence or nucleation in the real twin screw granulator system. This will be achieved by defining the relevant process kernels including, but not limited to, coalescence and breakage in an overarching population

Deleted:

Deleted:

Deleted:

Deleted:

balance framework. Once the granule size reaches or exceeds the minimum breakage size, x_{lc}, granule breakage is subject to the selection function $S = N * P_x$. Development of the full PB framework is beyond the scope of this paper, but the breakage kinetic model is presented in a way that makes its directly applicable within such a framework.

4.2 Breakage function (BF) development

The breakage function describes the size distribution of fragments and number of fragments in a single breakage event and, thus, is a key component in a population balance model. A detailed description of breakage functions proposed in the literature has been provided in [46].

4.2.1 Breakage size distribution in TSG

Figure 15 shows schematically the expected breakage functions for CEs (chipping) and DMEs (fragmentation). Chipping leads to a bimodal breakage function distribution where the large mode is only slightly smaller than the original particle size and the small mode represents the small chips or fines (Figure 15a). In contrast, fragmentation (Figure 15b) results in a wide range of particle sizes and a unimodal distribution with the mode in the breakage function distribution well below the original particle size.

Deleted:
Deleted:
Deleted:

Figure 15. A generic breakage size distribution for chipping in CEs and fragmentation in DMEs

4.2.2 Modified Weibull distribution in CEs and DMEs

Previous studies have used a simple breakage function for modelling TSGs, with the granule assumed to break into two halves with equal volume regardless of the applied stress [48]. The simplicity of such a breakage function limits the model's accuracy. However, the single particle breakage data presented here (Figure 8 and Figure 9) can be used to develop a more sophisticated breakage function. A modified Weibull distribution is proposed to describe the breakage fragment size distribution from DMEs via fragmentation,

Deleted:
Deleted:

$$B_x = 1 - \exp\left(-a * \left(\frac{x}{x_{uc}}\right)^b\right) \quad (9)$$

where B_x is the cumulative size distribution and a is the scale parameter and b is the shape parameter in the Weibull function.

To represent the distribution of coarse and fine particles that result from chipping in CEs, a bimodal distribution is proposed,

$$B_x = \nu B_{x1} + (1 - \nu) B_{x2} \tag{10}$$

where ν is the proportion of fine and coarse particles produced in Eq. (10) and B_{x1} and B_{x2} are the modified Weibull distributions identical in form to Eq. (9).

To test the accuracy of the proposed breakage function in Eq. (9) and Eq. (10), the fitting results of the breakage fragment size distributions of 3 mm granules, based on the breakage size distribution dataset in Figure 8 and Figure 9, are shown in Figure 16 and Figure 17. The results indicate that the modified Weibull distribution gives good agreement in both conveying and distributive mixing elements. The fitting parameters and goodness of fit are summarized in Table 4. The maximum breakage size x_{uc} is defined as 3.5 mm (rounded from 3.49 mm) and 3.2 mm (rounded from 3.18 mm). Note that there are extensive datasets of breakage particle distribution in the literature and, thus, it would be worthwhile to make a comprehensive assessment of the developed breakage functions against the literature data.

Figure 16. Modified Weibull prediction of breakage size distribution using conveying elements

Figure 17. Modified Weibull prediction of breakage size distribution using distributive mixing elements

Table 4. Fitting parameters of the modified Weibull distribution in the conveying and distributive mixing elements

Table 4 demonstrates that the two fitting parameters in the modified Weibull distribution are sufficient to produce a good fit to the experimental dataset. There may exist other breakage size distribution forms that fit the experimental data, but the proposed forms are accurate and simple to implement.

Deleted:
Deleted:
Deleted:
Deleted:
Deleted:
Deleted:

5 Parametric study

The input parameters in the proposed breakage kernels (selection function and breakage function) can be categorized into four types: material-dependent parameters (DYS and the minimum breakage size), a process-dependent parameter (PFN), screw-dependent parameters (maximum breakage size), and fitting parameters (a, b, and c). The parametric study in this work employs a univariate approach to quantifying the influence of the first three types of parameters on the selection and breakage functions. A reference case is first defined based on the breakage results from pellets. Next a univariate analysis of selected parameters is carried out and their influences on the selection function are summarized. In terms of the parametric study on the breakage function, the maximum breakage size in Eqs. (9) and (10) is employed for univariate analysis whereas the fitting parameters a, b, and v are kept constant with their values summarized in Table 4.

5.1 Reference parameters

Our reference case study is based on pellets as the reference material. The reference values for the input parameters are listed in Table 2 and Table 3. It should be noted that the CE and DME power exponents c must be arbitrarily specified in the current parametric study since experimental data sets for varying granule size in the range $x_{lc} < x < x_{uc}$ are not available. For pellet size 3 mm in CEs, we assume that the power exponent c is 2 in the expression $\hat{a} = a(x/x_{uc})^c$ giving a value of a = 0.4072 when $\hat{a} = 0.9162$. Likewise, for the lumped parameter $\hat{b} = b * \left(\frac{x}{x_{uc}}\right)^c$, the exponent c is assumed to be 10 giving a value of b = 0.0303 when the lumped parameter is $\hat{b} = 31.0142$. The fitting parameters a, b, and c are summarized in Table 5 based on the fitting of the data in Figure 3 and Figure 6. The maximum breakage size in CEs and DMEs are determined from the CAD model analysis, for which the data is shown in Figure 2 and Figure 5.

Table 5. The reference values of the input parameters for pellets in CEs and DMEs

The predicted breakage probabilities using Eq. (7) and Eq. (8) in a CE and DME, respectively, are depicted in Figure 18a and Figure 18b. Note that the symbols in Figures 18 (a) and 19(b) are experimental data for comparison to the proposed breakage model.

Deleted:
Deleted:
Deleted:
Deleted:
Deleted:
Deleted:
Deleted:
Deleted:
Deleted:

Figure 18. Breakage model prediction of pellet (a) in the conveying and (b) distributive mixing elements

The selection function is capable of predicting the effect of granule size on breakage probability irrespective of the breakage mode in different screw elements. However, the fitting curve with the input values in Table 5 is least accurate at the smallest breakage probability, which is consistent with the finding in Figure 14.

5.2 Influence of critical breakage size range

The critical breakage size range is bounded by the material-dependent minimum breakage size x_{lc} and the screw-dependent maximum breakage size x_{uc}. The variation for the minimum breakage size is chosen as ±20% of the reference value. The impact of varying x_{lc} for conveying elements between 1.6 and 2.4 mm on the breakage probability is shown in Figure 19a. The impact of varying x_{lc} for distributive mixing elements between 0.8 and 1.2 mm on the breakage probability is shown in Figure 19b. In the CE, there is relatively little breakage below x_{uc} and the breakage probability is insensitive to x_{lc}. In contrast, the predicted breakage probability is a strong function of x_{lc} for DMEs. This trend also occurs for different values of the exponent *c*.

Figure 19. Influence of minimum breakage size on breakage probability (a) in CE and (b) in DME

The maximum critical size is a geometry-defined parameter that is determined by the largest gap size through which the granule can pass. For comparative purposes, the variation for the maximum breakage size is chosen as ±20% of the reference value. Therefore, the ranges of maximum breakage size are chosen as 2.8 mm to 4.2 mm in the CE and 2.56 mm to 3.64 mm in the DME. The input values of fitting parameters a, b, and v are from Table 4. Figure 20 displays the influence of maximum breakage size on the cumulative granule size distributions in the CEs and DMEs.

Figure 20. Influence of maximum breakage size on the cumulative breakage size distribution (a) in CEs and (b) in DMEs

The plots indicate that the maximum critical size has a moderate effect on the breakage function. Increasing the maximum critical size moderately increases the proportion of larger granules. However, the increase of maximum critical size in CEs has a bigger influence on the larger particles than the fine particles.

5.3 Influence of PFN

The PFN is a function of powder feed rate, powder bulk density, shaft angular velocity, and the barrel diameter. The influence of PFN on the granule size distribution was found to be minor for the granule size distribution D_{10} and $D_{50,}$ but statistically significant for D_{90} [49]. The influence of PFN on the breakage probability in the CE and DME is shown in Figure 21a and Figure 21b. Increasing PFN results in increasing breakage probability in both the CE and DME. The influence of PFN on the breakage probability is more pronounced in the DME, which is consistent with the observation from the breakage specific experiments.

Figure 21. Influence of PFN on the breakage probability (a) in CE and (b) in DME

5.4 Influence of DYS

The DYS of material is an important indicator affecting granule deformation in a TSG [5, 44]. There exists a threshold of DYS above which the granule breakage is merely dependent on the screw geometry (approximately 9 kPa in the current work). The influence of DYS on the breakage probability in CEs and DMEs is shown in Figure 22a and Figure 22b, respectively. It is found that the DYS plays a negative role on the breakage probability in both the CE and DME. The breakage propensity in the DME is much larger than that in the CE using the same value of the DYS. In particular, the breakage probability of a pellet with a 9 kPa DYS is nearly zero in the CE regardless of the pellet size. However, the breakage probability of a pellet with a DYS equal to 9 kPa increases to 100% when the pellet size increases to 3 mm.

Figure 22. Influence of DYS on breakage probability (a) in CE and (b) in DME

The influences of minimum breakage size, maximum breakage size, DYS, and PFN on the selection function and the breakage function are summarized in Table 6.

Table 6. Influence of input parameters on the developed breakage kernel

It should be noted that interactive effects play an important role in the final granule attributes, which cannot be achieved by OAT (one-at-a-time) analysis. However, as a prelude to explore the interactive effects of the parameters in a PBM, OAT analysis serves to identify the effects of individual parameters on the final attribute by singling out the most influential parameters.

A Global System Analysis (GSA) is a valuable tool for an interactive analysis, but it is not considered here due to the research scope in this paper. However, a GSA for the PBM parameters is currently under investigation by incorporating the new breakage models in a PBM modelling package for TSG.

6 Discussion

A breakage kernel in the population balance modelling of a TSG was developed based on breakage specific experiments. The advantages of the developed kernel include the influence of different screw elements, the piecewise breakage probability based on the critical breakage size, and the incorporation of key parameters such as DYS and PFN. However, several issues remain to be addressed:

1. The breakage specific experiments demonstrate that the breakage probability increases with an increase in PFN and a decrease in DYS. Although the effect of PFN and DYS are incorporated in the developed selection function, the challenge in the breakage model development is whether it is possible to develop a unified selection function accounting for both chipping and fragmentation in different screw elements.

2. Although the modified Weibull distribution was developed to describe the breakage size distribution, further efforts are required to provide insights between the two Weibull parameters and mechanical property (DYS) as well as the process parameter PFN. There are many breakage functions in the literature and their applicability in TSG has not yet been fully tested. The majority of the breakage functions display a mono-modal distribution of breakage particle size while less attention is given to bi-modal distributions. A comprehensive assessment of mono-modal and bi-modal size distributions will be valuable for the practical guide of defining the most appropriate breakage selection in PBM.

3. The breakage specific experiments in TSG were carried out in CEs and DMEs. Due to the discrete nature of the particle size, the chipping data of a granule between 3.0 mm and 3.49

mm is unavailable. Moreover, there is no literature data available for breakage-isolated experiments for CEs. In the current work, arbitrary but reasonable input values were assumed for the exponent c in the CE and DME breakage probability functions. Additional breakage specific experiments of varying particle size are still required to validate this assumption. Breakage-isolated experiments in kneading elements (KEs) should also be carried out to investigate the applicability of the developed breakage kernel as KEs are a key screw element widely used in TSGs.

4. The parametric study of the input parameters in the developed breakage kernel indicates that the influence of DYS and PFN on the selection function is more pronounced in a DME compared to a CE. However, the influence of these input parameters on the granule product attributes in the context of PBM are not yet fully identified and a systematic analysis of the input parameters in the rate process kernels is still scarce. The category of the PBM input parameters should also be clarified to reduce the modelling uncertainty. Hence, a global sensitivity analysis of full factorial parameters in the rate process kernels should be performed to identify the significance of each parameter on the granule product attributes.

7 Conclusions

This paper has presented the breakage kernel development in the population balance modelling of twin screw granulation. It was found that the breakage probability increases with an increase in PFN and a decrease of DYS. The breakage probability is dependent on the screw geometry for material DYS values smaller than a threshold value (9 kPa), but independent of DYS and geometry above DYS = 9kPa. There exists a material dependent parameter, the minimum breakage size (x_{lc}), below which no breakage occurs and a screw geometry dependent parameter, the maximum breakage size (x_{uc}), above which all granules are broken. The breakage of particles takes place between the minimum breakage size and the maximum breakage size and the breakage size regime ($x_{uc} - x_{lc}$) is typically broader in DMEs than that in CEs.

A piecewise breakage selection function was used to describe the breakage probability in CEs and DMEs taking into account the material dependent parameters (DYS, granule size, and minimum breakage size), the process parameter PFN, and the screw dependent parameter (maximum breakage size). The selection function gave very good agreement with

the experimental observations in both the CEs and DMEs. A modified Weibull distribution was used to describe the breakage size distribution for DMEs and gave a good fit to experimental data. For CEs, a bimodal breakage size distribution was required to describe the experimental data, reflecting that chipping is the predominant breakage mechanism for CEs.

This work presents the first breakage model specifically developed for a TSG and incorporates a mechanistic understanding of the process, particularly the role of screw geometry. The model is suitable for incorporating into a population balance framework to describe twin screw granulation.

8 Nomenclature

a	Fitting parameter, -
b_M	Breakage function, -
$B(v,t)$	Birth rate, $m^{-3}s^{-1}$
B_{break}	Birth rate of breakage, $m^{-3}s^{-1}$
B_{lay}	Birth rate of layering, $m^{-3}s^{-1}$
B_{nuc}	Birth rate of nucleation, $m^{-3}s^{-1}$
c	Fitting parameters, -
D	Screw diameter, mm
$D(v,t)$	Death rate, $m^{-3}s^{-1}$
D_{break}	Death rate of breakage, $m^{-3}s^{-1}$
$D_{m_p,nuc}$	Death rate of powder particles, kg $m^{-3}s^{-1}$
$M(v,t)$	Mass of granule with volume v at time t, kg
$\dot{m}_{powder}$	Feed rate of powder, kg/h

n	Population density of length function, m^{-3}
N	Number of breakage events, -
P_x	Breakage probability of particle size x, -
S	Breakage rate, s^{-1}
x	Particle size, mm
x_{lc}	Minimum breakage size, mm
x_{uc}	Maximum breakage size, mm
v	Proportion of fines and granules, -
ω	Angular velocity of the shaft, $rads^{-1}$
ρ_{bulk}	Particle bulk density, kg m^{-3}
DYS	Dynamic yield strength, kPa
LSR	Liquid solid ratio,-
PFN	Powder feed number,-

Acknowledgement

The writers gratefully acknowledge the financial support from Centre for Process Innovation (CPI) for research under the project of Models for Manufacturing of Particulate Products. We would like to thank all the partners from the sponsors including AstraZeneca, CPI, EDEM (DEM Solutions Ltd.), Johnson Matthey, Pfizer, Procter & Gamble, PSE (Process Systems Enterprise), and the University of Edinburgh for their feedback and many helpful discussions.

Appendix

To support the conclusion that the influence of PFN is more pronounced for weaker materials and in DMEs as compared to CEs, an ANOVA analysis was carried out to corroborate the conclusion stated in this paper. The breakage probability subject to varying

DYS and PFN values are shown in Table A1 for CEs and Table A2 for DMEs, respectively. The ANOVA analysis was performed based on the data in Tables A1 and A2.

Table A1 Breakage probability of pellet (3 mm) subject to varying DYS and PFN in DME

DYS (kPa) \ PFN	Breakage probability		
	0.011	0.022	0.045
12.38899	0	0	0
8.49463	0.125	0	0.05
5.16542	0.15	0.15	0.225
2.25964	0.125	0.25	0.45
1.27398	0.125	0.35	0.675

Table A2 Breakage probability of pellet (2 mm) subject to varying DYS and PFN in DME

DYS (kPa) \ PFN	Breakage probability		
	0.011	0.022	0.045
12.38899	0.125	0.225	0.15
8.49463	0.1	0.275	0.2
5.16542	0.1	0.325	0.35
2.25964	0.15	0.375	0.55
1.27398	0.15	0.475	0.65

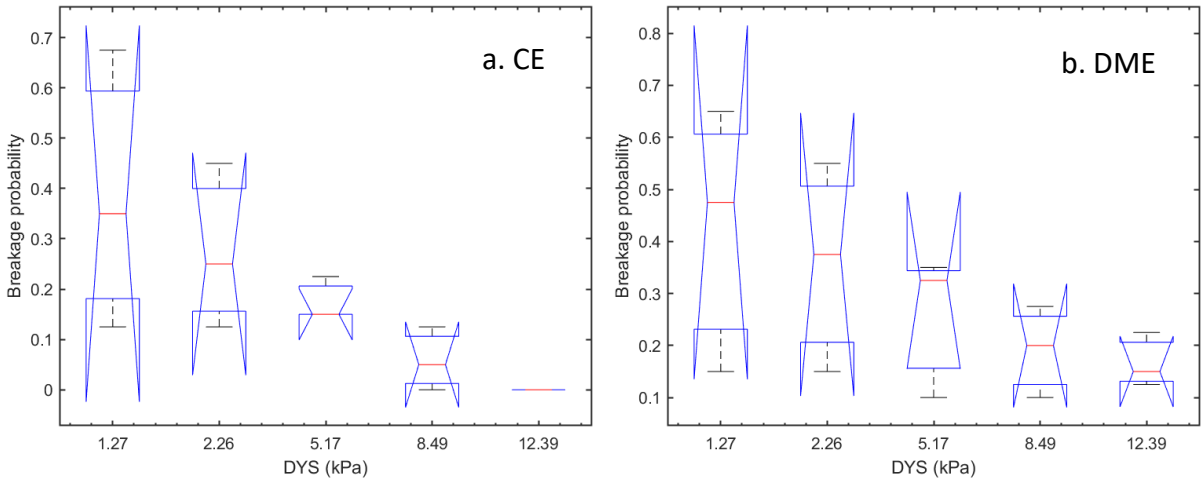

Figure A1 Comparison of Kruskal-Wallis ANOVA analysis of PFN subject to varying DYS in (a) CE and (b) DME

References

[1] R.M. Dhenge, K. Washino, J.J. Cartwright, M.J. Hounslow, A.D. Salman, Twin screw granulation using conveying screws: Effects of viscosity of granulation liquids and flow of powders, Powder Technol. 238 (2013) 77–90. doi:10.1016/j.powtec.2012.05.045.

[2] A.S. El Hagrasy, J.R. Hennenkamp, M.D. Burke, J.J. Cartwright, J.D. Litster, Twin screw wet granulation: Influence of formulation parameters on granule properties and growth behavior, Powder Technol. 238 (2013) 108–115. doi:10.1016/J.POWTEC.2012.04.035.

[3] T.C. Seem, N.A. Rowson, A. Ingram, Z. Huang, S. Yu, M. de Matas, I. Gabbott, G.K. Reynolds, Twin Screw Granulation – A Literature Review, Powder Technol. 276 (2015) 89–102. doi:10.1016/j.powtec.2015.01.075.

[4] J. Li, S.U. Pradhan, C.R. Wassgren, Granule transformation in a twin screw granulator: Effects of conveying, kneading, and distributive mixing elements, Powder Technol. 346 (2019) 363–372. doi:10.1016/J.POWTEC.2018.11.099.

[5] S.U. Pradhan, M. Sen, J. Li, J.D. Litster, C.R. Wassgren, Granule Breakage in Twin Screw Granulation: Effect of Material Properties and Screw Element Geometry, Powder Technol. 315 (2017) 290–299. doi:10.1016/j.powtec.2017.04.011.

[6] R. Sayin, A.S. El Hagrasy, J.D. Litster, Distributive mixing elements: Towards improved granule attributes from a twin screw granulation process, Chem. Eng. Sci. 125 (2015) 165–175. doi:10.1016/j.ces.2014.06.040.

[7] M.R. Thompson, J. Sun, Wet granulation in a twin-screw extruder: implications of screw design, J. Pharm. Sci. 99 (2010) 2090–2103. doi:10.1002/jps.21973.

[8] D. Djuric, P. Kleinebudde, Impact of screw elements on continuous granulation with a twin-screw extruder, J. Pharm. Sci. 97 (2008) 4934–4942. doi:10.1002/jps.21339.

[9] H. Li, M.R. Thompson, K.P. O'Donnell, Understanding wet granulation in the kneading block of twin screw extruders, Chem. Eng. Sci. 113 (2014) 11–21. doi:10.1016/j.ces.2014.03.007.

[10] A.S. El Hagrasy, J.D. Litster, Granulation rate processes in the kneading elements of a twin screw granulator, AIChE J. 59 (2013) 4100–4115. doi:10.1002/aic.14180.

[11] R.M. Dhenge, J.J. Cartwright, M.J. Hounslow, A.D. Salman, Twin screw granulation: Steps in granule growth, Int. J. Pharm. 438 (2012) 20–32. doi:10.1016/j.ijpharm.2012.08.049.

[12] M. Maniruzzaman, S.A. Ross, T. Dey, A. Nair, M.J. Snowden, D. Douroumis, A quality by design (QbD) twin—Screw extrusion wet granulation approach for processing water insoluble drugs, Int. J. Pharm. 526 (2017) 496–505. doi:10.1016/J.IJPHARM.2017.05.020.

[13] S.U. Pradhan, M. Sen, J. Li, I. Gabbott, G. Reynolds, J.D. Litster, C.R. Wassgren, Characteristics of multi-component formulation granules formed using distributive mixing elements in twin screw granulation, Drug Dev. Ind. Pharm. 44 (2018) 1826–1837. doi:10.1080/03639045.2018.1503293.

[14] M.R. Thompson, Twin screw granulation – review of current progress, Drug Dev. Ind. Pharm. 41 (2015) 1223–1231. doi:10.3109/03639045.2014.983931.

[15] S.U. Pradhan, Y. Zhang, J. Li, J.D. Litster, C.R. Wassgren, Tailored granule properties using 3D printed screw geometries in twin screw granulation, Powder Technol. (2018). doi:10.1016/j.powtec.2017.12.068

[16] M. Fonteyne, A. Correia, S. De Plecker, J. Vercruysse, I. Ilić, Q. Zhou, C. Vervaet, J.P. Remon, F. Onofre, V. Bulone, T. De Beer, Impact of microcrystalline cellulose material attributes: A case study on continuous twin screw granulation, Int. J. Pharm. 478 (2015) 705–717. doi:10.1016/j.ijpharm.2014.11.070.

[17] E.I. Keleb, a. Vermeire, C. Vervaet, J.P. Remon, Continuous twin screw extrusion for the wet granulation of lactose, Int. J. Pharm. 239 (2002) 69–80. doi:10.1016/S0378-5173(02)00052-2.

[18] E.I. Keleb, A. Vermeire, C. Vervaet, P.D.J.P. Remon, Extrusion Granulation and High Shear Granulation of Different Grades of Lactose and Highly Dosed Drugs: A Comparative Study, Drug Dev. Ind. Pharm. (2004).

[19] K.T. Lee, A. Ingram, N.A. Rowson, Comparison of granule properties produced using Twin Screw Extruder and High Shear Mixer: A step towards understanding the mechanism of twin screw wet granulation, Powder Technol. 238 (2013) 91–98. doi:10.1016/j.powtec.2012.05.031.

[20] H. Li, M.R. Thompson, K.P. O'Donnell, Examining Drug Hydrophobicity in Continuous Wet Granulation within a Twin Screw Extruder, Int. J. Pharm. 496 (2015) 3–11. doi:10.1016/j.ijpharm.2015.07.070.

[21] S. V. Lute, R.M. Dhenge, M.J. Hounslow, A.D. Salman, Twin screw granulation: Understanding the mechanism of granule formation along the barrel length, Chem. Eng. Res. Des. 110 (2016) 43–53. doi:10.1016/j.cherd.2016.03.008.

[22] R. Meier, M. Thommes, N. Rasenack, M. Krumme, K.-P. Moll, P. Kleinebudde, Simplified formulations with high drug loads for continuous twin-screw granulation, Int. J. Pharm. (2015). doi:10.1016/j.ijpharm.2015.05.060.

[23] J.G. Osorio, R. Sayin, A. V. Kalbag, J.D. Litster, L. Martinez-Marcos, D.A. Lamprou, G.W. Halbert, Scaling of continuous twin screw wet granulation, AIChE J. 63 (2017) 921–932. doi:10.1002/aic.15459.

[24] M.F. Saleh, R.M. Dhenge, J.J. Cartwright, M.J. Hounslow, A.D. Salman, Twin screw wet granulation: Effect of process and formulation variables on powder caking during production, Int. J. Pharm. 496 (2015) 571–582. doi:10.1016/J.IJPHARM.2015.10.069.

[25] M.F. Saleh, R.M. Dhenge, J.J. Cartwright, M.J. Hounslow, A.D. Salman, Twin screw wet granulation: Binder delivery, Int. J. Pharm. 487 (2015) 124–134. doi:10.1016/j.ijpharm.2015.04.017.

[26] M.R. Thompson, S. Weatherley, R.N. Pukadyil, P.J. Sheskey, Foam granulation: new developments in pharmaceutical solid oral dosage forms using twin screw extrusion machinery, Drug Dev. Ind. Pharm. 38 (2012) 771–784.

[27] V. Vanhoorne, B. Vanbillemont, J. Vercruysse, F. De Leersnyder, P. Gomes, T. De Beer, J.P. Remon, C. Vervaet, Development of a controlled release formulation by continuous twin screw granulation: Influence of process and formulation parameters, Int. J. Pharm. 505 (2016) 61–68. doi:10.1016/j.ijpharm.2016.03.058.

[28] J. Vercruysse, D. Córdoba Díaz, E. Peeters, M. Fonteyne, U. Delaet, I. Van Assche, T. De Beer, J.P. Remon, C. Vervaet, Continuous twin screw granulation: Influence of process variables on granule and tablet quality, Eur. J. Pharm. Biopharm. 82 (2012) 205–211. doi:10.1016/j.ejpb.2012.05.010.

[29] N. Willecke, A. Szepes, M. Wunderlich, J.P. Remon, C. Vervaet, T. De Beer, Identifying overarching excipient properties towards an in-depth understanding of process and product performance for continuous twin-screw wet granulation, Int. J. Pharm. 522 (2017) 234–247. doi:10.1016/j.ijpharm.2017.02.028.

[30] S. Yu, G.K. Reynolds, Z. Huang, M. de Matas, A.D. Salman, Granulation of increasingly hydrophobic formulations using a twin screw granulator., Int. J. Pharm. 475 (2014) 82–96. doi:10.1016/j.ijpharm.2014.08.015.

[31] R.M. Dhenge, J.J. Cartwright, D.G. Doughty, M.J. Hounslow, A.D. Salman, Twin screw wet granulation: Effect of powder feed rate, Adv. Powder Technol. 22 (2011) 162–166. doi:10.1016/j.apt.2010.09.004.

[32] R.M. Dhenge, J.J. Cartwright, M.J. Hounslow, A.D. Salman, Twin screw wet granulation: Effects of properties of granulation liquid, Powder Technol. 229 (2012) 126–136. doi:10.1016/j.powtec.2012.06.019.

[33] R.M. Dhenge, R.S. Fyles, J.J. Cartwright, D.G. Doughty, M.J. Hounslow, A.D. Salman, Twin screw wet granulation: Granule properties, Chem. Eng. J. 164 (2010) 322–329. doi:10.1016/j.cej.2010.05.023.

[34] D. Djuric, P. Kleinebudde, Continuous granulation with a twin-screw extruder: Impact of material throughput, Pharm. Dev. Technol. (2010).

[35] S.M. Iveson, J.A. Beathe, N.W. Page, The dynamic strength of partially saturated powder compacts: the effect of liquid properties, Powder Technol. 127 (2002) 149–161. doi:10.1016/S0032-5910(02)00118-3.

[36] S.M. Iveson, N.W. Page, Brittle to Plastic Transition in the Dynamic Mechanical Behavior of Partially Saturated Granular Materials, J. Appl. Mech. 71 (2004) 470. doi:10.1115/1.1753269.

[37] S.M. Iveson, N.W. Page, Dynamic strength of liquid-bound granular materials: The effect of particle size and shape, Powder Technol. 152 (2005) 79–89. doi:10.1016/j.powtec.2005.01.020.

[38] M.K. Paavola, A.S. El-Hagrasy, J.D. Litster, K.J. Leiviska, 3D Population Balance Model for Continuous Twin Screw Granulator, Icheap-11 11Th Int. Conf. Chem. Process Eng. Pts 1-4. 32 (2013) 2077–2082. doi:10.3303/CET1332347.

[39] D. Barrasso, A. El Hagrasy, J.D. Litster, R. Ramachandran, Multi-dimensional population balance model development and validation for a twin screw granulation process, Powder Technol. 270 (2015) 612–621. doi:10.1016/j.powtec.2014.06.035.

[40] A. Kumar, J. Vercruysse, S.T.F.C. Mortier, C. Vervaet, J.P. Remon, K. V. Gernaey, T. De Beer, I. Nopens, Model-based analysis of a twin-screw wet granulation system for continuous solid dosage manufacturing, Comput. Chem. Eng. 89 (2016) 62–70. doi:10.1016/j.compchemeng.2016.03.007.

[41] H. Liu, S.C. Galbraith, S.-Y. Park, B. Cha, Z. Huang, R.F. Meyer, M.H. Flamm, T. O'Connor, S. Lee, S. Yoon, Development of a three-compartmental population balance model for a continuous twin screw wet granulation process, Pharm. Dev. Technol. 0 (2018) 1–39. doi:10.1080/10837450.2018.1427106.

[42] J.M.-H. Poon, C.D. Immanuel, F.J. Doyle, III, J.D. Litster, A three-dimensional population balance model of granulation with a mechanistic representation of the nucleation and aggregation phenomena, Chem. Eng. Sci. 63 (2008) 1315–1329. doi:10.1016/j.ces.2007.07.048.

[43] P.J. Hill, K.M. Ng, New discretization procedure for the breakage equation, AIChE J. 41 (1995) 1204–1216. doi:10.1002/aic.690410516.

[44] S.U. Pradhan, Quality by design in twin screw granulation, Purdue University, 2017.

[45] J. Litster, B.J. Ennis, Ennis, Litster - The Science and Engineering of Granulation Processes, 2004.

[46] L.G. Wang, Particle Breakage Mechanics in Milling Operation, University of Edinburgh, 2016.

[47] R. Sayin, Mechanistic studies of twin screw granulation, Purdue University, 2016.

[48] D. Barrasso, R. Ramachandran, Qualitative Assessment of a Multi-Scale, Compartmental PBM-DEM Model of a Continuous Twin-Screw Wet Granulation Process, J. Pharm. Innov. 11 (2016) 231–249. doi:10.1007/s12247-015-9240-7.

[49] J. Osorio, Scaling of Continuous Twin Screw Wet Granulation, Am. Inst. Chem. Eng. 63 (2016) 921–932. doi:10.1002/aic.

[50] R. M. Smith, L. X. Liu, J. D. Litster, Breakage of drop nucleated granules in a breakage only high shear mixer, Chem. Eng. Sci. 65 (2010) 5651-5657, doi: 10.1016/j.ces.2010.06.037.

[51] R. M. Smith, Wet Granule Breakage in High Shear Mixer Granulators, University of Queensland (2007).